Inflammation Research (2026) 75:71
https://doi.org/10.1007/s00011-026-02200-1

Inflammation Research

RESEARCH

# Proteomic profiling and pathway analyses reveal molecular signatures and immune networks in pediatric sepsis

Vincenzo Stranges[1] · Logan R. Van Nynatten[2,3] · David Tweddell[4] · Enis Cela[3] · Maria Morello[5] · Mark Daley[4,6] · David B. O'Gorman[7] · Gediminas Cepinskas[8,9,10] · Douglas D. Fraser[3,10,11,12,13,14]

Received: 11 December 2025 / Revised: 27 January 2026 / Accepted: 2 February 2026


## Abstract

**Background** Sepsis remains a leading cause of childhood mortality worldwide. Most deaths occur within the first few days of presentation, underscoring the urgent need for early recognition and biologically informed treatment strategies. The heterogeneous etiology of sepsis involves complex, intertwined biological networks, explaining why single-biomarker approaches have proven inadequate for capturing this complexity. We used high-throughput proximity extension assay technology to comprehensively profile plasma proteins in critically ill pediatric sepsis patients, aiming to identify dysregulated biological pathways that could inform risk stratification and therapeutic development.

**Methods** Study participants were prospectively enrolled based on established pediatric sepsis criteria. Plasma proteins were quantified using the Olink proximity extension assay, with differential expression, machine learning, and pathway enrichment analyses performed to define molecular signatures of pediatric sepsis.

**Results** Analysis of plasma samples from 17 pediatric sepsis patients and 17 age- and sex-matched healthy controls revealed 626 significantly differentially expressed proteins: 399 upregulated and 227 downregulated. The most significantly elevated proteins included calcitonin-related polypeptide α (CALCA), tumor necrosis factor superfamily member 14 (TNFSF14), and asialoglycoprotein receptor 1 (ASGR1). Machine learning identified a minimal 9-protein signature accounting for 90% of discriminatory power between groups. Pathway enrichment analysis revealed profound dysregulation of immune and inflammatory networks. Interleukin-10 (IL-10) signaling emerged as the most significantly enriched pathway, alongside extracellular matrix degradation, IL-4 and IL-13 signaling, and other cytokine signaling pathways. Dysregulated pathways were associated with clinical variables, particularly gram-negative infections and respiratory infection sources.

**Conclusions** Pediatric sepsis is characterized by dysregulation of multiple immune and inflammatory pathways rather than isolated protein abnormalities. IL-10 and related cytokine signaling emerged as central nodes, providing insights into the balance between hyperinflammation and immunosuppression in critically ill children. Associations between pathways and clinical variables suggest that specific pathogen types and infection sources trigger distinct patterns of biological network activation, offering potential targets for patient stratification and pathway-directed therapeutics.

**Keywords** Pediatric · Sepsis · Proteomics · Bioinformatics · Critical care

**Abbreviations**

| | |
|---|---|
| PICU | Pediatric intensive care unit |
| PRISM III | Pediatric risk of mortality III |
| PIM-2 | Pediatric index of mortality 2 |
| PELOD-2 | Pediatric logistic organ dysfunction 2 |

**Methodological abbreviations**

| | |
|---|---|
| GCS | Glasgow coma scale |
| PEA | Proximity extension assay |
| NPX | Normalized protein expression |
| qPCR | Quantitative polymerase chain reaction |
| IQR | Interquartile range |
| FDR | False discovery rate |

Communicated by Janos G Filep

Extended author information available on the last page of the article

Published online: 27 March 2026

| | |
|---|---|
| ORA | Over-representation analysis |
| GSEA | Gene set enrichment analysis |
| GO | Gene ontology |
| DEP | Differentially expressed protein |
| RFC | Random forest classifier |
| ETC | Extremely randomized trees classifier |
| GBC | Gradient boosting classifier |
| t-SNE | T-distributed stochastic neighbor embedding |
| ES | Enrichment score |
| NES | Normalized enrichment score |
| OR | Odds ratio |
| PCA | Principal component analysis |

**Immunological and molecular terms**

| | |
|---|---|
| NET | Neutrophil extracellular trap |
| ECM | Extracellular matrix |
| MMP | Matrix metalloproteinase |
| GH | Growth hormone |
| IGF | Insulin-like growth factor |
| IGFBP | Insulin-like growth factor binding protein |
| PI3K | Phosphoinositide 3-Kinase |
| GPCR | G Protein-coupled receptor |

**Protein abbreviations**

| | |
|---|---|
| CALCA | Calcitonin-related polypeptide alpha |
| CGRP | Calcitonin gene-related peptide |
| PCT | Procalcitonin |
| TNFSF | Tumor necrosis factor superfamily |
| TNFRSF | Tumor necrosis factor receptor superfamily |
| ASGR | Asialoglycoprotein receptor |
| CTSV | Cathepsin V |
| IL | Interleukin |
| TNF | Tumor necrosis factor |
| CRP | C-Reactive protein |
| IFNG | Interferon gamma |
| CXCL | C-X-C motif chemokine ligand |
| CCL | Chemokine ligand |
| FAP | Fibroblast activation protein |
| IL-4R | Interleukin-4 receptor |
| RGMA | Repulsive guidance molecule A |
| NK | Natural killer |
| TRAIL | TNF-related apoptosis-inducing ligand |
| NF-κB | Nuclear factor Kappa B |
| ARDS | Acute Respiratory Distress Syndrome |
| COVID-19 | Coronavirus Disease 2019 |
| SARS-CoV-2 | Severe Acute Respiratory Syndrome Coronavirus 2 |

## Background

Sepsis is a life-threatening syndrome characterized by a dysregulated host response to infection that leads to organ dysfunction and, in severe cases, shock and death [1]. It remains a major global health threat, contributing to an estimated 3.3 million pediatric deaths each year [2]. Reported mortality rates in children with sepsis range from 4 to 50% depending on illness severity, comorbid risk factors, and geographic context, with most deaths occurring in the first 48–72 h after presentation [3]. These early, high-risk trajectories underscore the urgent need for timely recognition and biologically informed management strategies in pediatric sepsis.

The initial immune response to invading pathogens is mediated by pattern-recognition receptors that detect pathogen-associated molecular patterns (PAMPs). When infection control fails, the host response can become maladaptive, where excessive inflammation coexists with profound immune suppression, with damaged host cells releasing damage-associated molecular patterns (DAMPs) that perpetuate innate immune system activation [4, 5]. This cascade triggers cytokine and chemokine release, acute-phase protein production, complement activation, coagulation disturbances, endothelial barrier injury, fibrinolytic shutdown, and metabolic reprogramming [6, 7]. It is the activation of multiple, intertwined networks, rather than a single linear pathway, that drives the heterogeneous clinical manifestations and outcomes of sepsis.

Measurable indicators of normal or pathological responses to disease or therapy, i.e., biomarkers, are attractive tools for improving sepsis diagnosis, risk stratification, and therapeutic targeting [8–11]. However, the biological complexity of sepsis and developmental differences between children and adults can confound fixed thresholds and reference ranges. High-throughput proteomics offers a more comprehensive alternative by simultaneously quantifying thousands of circulating proteins and capturing network-level dysregulation [12, 13]. These approaches have helped establish and validate biomarker panels as prognostic indicators for critically ill pediatric patients with sepsis [14–17]. Platforms such as proximity extension assays (PEAs), aptamer-based profiling, and mass spectrometry provide comprehensive assessments of proteomic and metabolic pathways [18], while modern bioinformatics and enrichment analyses, such as Gene Ontology (GO) over-representation analysis (ORA) and Gene Set Enrichment Analysis (GSEA), can reveal biologically coherent molecular modules that are far more informative than isolated biomarkers [19–21].

Accordingly, the primary objective of this study was to use high-throughput PEA technology to broadly characterize the pediatric sepsis proteome and to identify proteins

that are differentially expressed in patients with sepsis compared to healthy control subjects. Secondary objectives included: (1) performing pathway-level analyses to identify dysregulated pathways characterizing sepsis pathobiology and (2) investigating associations of dysregulated pathways with clinical parameters and outcomes.

## Methods

### Study participants and blood sampling

This was an exploratory case-control cohort study in which we used high-throughput proteomic profiling of plasma samples from critically ill pediatric patients with sepsis, combined with bioinformatic analysis to gain novel insights into disease pathobiology. The study was approved by the Human Research Ethics Board of Western University. All procedures involving human participants were conducted in accordance with the ethical standards of the responsible committee and the principles of the Declaration of Helsinki (1975). Written informed consent was obtained from the legal guardians of all pediatric patients admitted to the PICU with sepsis, and assent and consent were obtained for all healthy control participants as appropriate.

Pediatric Intensive Care Unit (PICU) patients were enrolled prospectively via convenience sampling approach according to the International Consensus Criteria for Pediatric Sepsis and Septic Shock criteria [22], between 2010 and 2019. Patients who also met the more recent pediatric consensus sepsis criteria [2, 23] were selected for use in this study. Patients were excluded if they were greater than 18 years of age, if sepsis was not the sole/presenting diagnosis, or if consent was not obtained. The cohort consisted of 34 age- and sex-matched subjects (17 critically ill pediatric patients with sepsis, 17 healthy control subjects). Patient demographics, including age, sex, and comorbidities, were collected. Additional clinical characteristics, including infecting pathogen, infection source, chest x-ray findings, and clinical outcomes, including non-invasive or invasive mechanical ventilation, use of hemodynamic support, length of ICU stay, and length of hospital stay, were also collected. Severity of illness was assessed using the Pediatric Risk of Mortality III (PRISM III), Pediatric Index of Mortality 2 (PIM-2), daily Pediatric Logistic Organ Dysfunction 2 (PELOD-2), and the Glasgow Coma Scale (GCS). All patients were treated with similar institutional practices, although antibiotic choice and fluid resuscitation targets were at the discretion of the intensivist.

Blood samples were collected within 24 h of admission to PICU, specifically for research purposes. Samples were drawn into vacutainer blood collection tubes containing sodium citrate, and were immediately processed by centrifugation at 1500 × g for 15 min at 4 °C. The plasma was isolated, aliquoted, and stored at − 80 °C. Freeze-thaw cycles were avoided. For comparison, age- and sex-matched healthy control subjects without any acute illness or disease were selected from the Translational Research Centre in London, Ontario (www.translationalresearch.ca) [24, 25]. The plasma samples from healthy controls were processed and stored in the same manner as those from sepsis patients.

### Proximity extension assay (PEA)

Circulating plasma proteins were measured using PEAs capable of detecting and identifying 1472 proteins (Olink 1472) following established protocols [26, 27]. In brief, PEAs have three main steps: (1) binding of antibody pairs, each tagged with complementary DNA oligonucleotides encoding unique barcodes, to target protein antigens in the plasma; (2) hybridization of the complementary oligonucleotides and duplex extension by DNA polymerase; and (3) amplification of the resulting DNA duplexes, including the unique barcode identifying the protein target, by quantitative polymerase chain reaction (qPCR). Results were reported as relative quantification on a $\log_2$ scale of normalized protein expression (NPX) values. Quality controls to assess sample quality, immunoassay performance, and detection efficiency were included.

### Metadata analysis and quality control

A total of 34 samples were collected and assessed from 34 patients, consisting of 17 sepsis patients and 17 healthy controls, at a single time point. Age and sex information was collated for all patients and additional metadata, such as comorbidities and the pathogen source, were collected for the sepsis patients. The complete metadata included 34 samples and 18 variables. After excluding variables unique to individual samples, 17 variables (10 categorical and 7 numeric) were included in subsequent analyses.

The potential for confounding factors in the experimental design was assessed by performing pairwise univariate association tests between all combinations. The choice of statistical test depended on the type of factors involved. For associations between two continuous factors, a Spearman correlation test was used. For associations between a survival factor (time and censoring) and a categorical factor, a Cox proportional hazards model was employed, with significance determined using the Wald test. In all cases, the resulting $p$ values were transformed as $-\log_{10}(p)$ before visualization in the corresponding heatmap.

Quality assessments of proteomic data were performed on all samples to identify outliers. A sample was considered

an outlier if it failed two or more of the following objective statistical criteria: Sum of Euclidean distance to other samples, Kolmogorov-Smirnov test statistic, Mean Pearson correlation with other samples, or Hoeffding's D statistic. Data were visually interrogated using principal component analysis and kernel density estimates to visually identify outliers. Two samples (both sepsis patients) were excluded after failing quality assessment.

## Conventional statistics

Cohort demographic and clinical characteristics were collected as described. Continuous variables were reported as medians with interquartile ranges (IQRs), and categorical variables as counts (n) with percentages (%). Normalized proteomic data were used to identify plasma proteins that differed significantly between sepsis patients and healthy control subjects. Statistical comparisons were conducted using empirical Bayes moderated t-tests. A statistical threshold of false discovery rate (FDR)-adjusted $p < 0.05$ was used to define significantly different protein levels. Volcano plots were generated to visualize fold changes, such that a positive $\log_2$ (fold change) was selected to indicate up-regulation in sepsis patients relative to healthy controls and a negative $\log_2$ value indicated the downregulation in sepsis patients relative to controls.

## Machine learning and feature selection

To identify predictive protein biomarkers from high-dimensional data, we evaluated three ensemble decision tree classifiers: (1) Random Forest Classifier (RFC) [28], (2) Extremely Randomized Trees Classifier (ETC) [29], and (3) Gradient Boosting Classifier (GBC) [30]. These were combined with Boruta feature selection [31] to identify the features (proteins) best able to identify class membership (scikit-learn version 1.6). Each patient's protein expression profile was represented as a 1463-dimensional feature vector derived from 1472 proteins after averaging and resolving of duplicated protein features. GBC was selected as the optimal classifier based on its parsimony in feature selection and computational efficiency, and was combined with Boruta feature selection (Boruta-py version 0.4.3) [31] to identify important features in sepsis patients versus healthy controls. High-dimensional data were visualized using t-SNE projection into 2D space. Due to limited sample size, model performance was assessed through feature stability analysis rather than traditional cross-validation.

## Reactome pathway ORA enrichment

Input proteins that were up- or down-regulated in sepsis patients compared to healthy controls, meeting an adjusted $p$ value $< 0.05$ and a fold change $\geq 2.5$, were mapped to Entrez gene identifiers and assessed using Reactome pathway over-representation analysis (ORA). Reactome (package: reactome.db (v)) is based on the hierarchical grouping of known reactions, such as bindings, reactions, or modifications, between proteins. Enrichment analysis was completed using the clusterProfiler package, specifying a minimum set size of 10 and a maximum set size of 500. These parameters indicated the minimum and maximum number of proteins in a Reactome pathway to be tested for over-representation.

Reactome pathway enrichment was assessed using over-representation analysis to determine whether significantly differentially expressed proteins were enriched within individual pathways beyond what would be expected by chance. Statistical significance was evaluated using the hypergeometric test implemented in clusterProfiler, with $p$ values adjusted for multiple testing using the Benjamini-Hochberg method. Pathways with adjusted $p$ values $< 0.05$ were considered significantly enriched. Odds ratios (OR) were calculated as a ratio of the observed to expected differentially expressed proteins per pathway. Pathway directional activity was assessed using Z-scores calculated as $Z = (S_u - S^d)/\sqrt{N}$, where N is the total number of proteins in the pathway, and $S_u$ and $S^d$ represent the number of significantly up-regulated and down-regulated proteins, respectively.

## Reactome pathway GSEA enrichment

To corroborate the findings of the ORA Reactome enrichment, gene set enrichment analysis (GSEA) was performed (fgsea R package) to determine whether sets of proteins involved in pathways of interest tended to be over-represented (enriched) at the extremes of an ordered list of proteins. This ordered list of proteins was created by ranking all proteins from high to low according to a statistic. The minimum gene set size tested was 15, and all pathways below this threshold were excluded. The maximum gene set size tested was 500, with all pathways above this threshold excluded. The statistical significance (nominal $p$ value) of the over-representation was evaluated using a method based on an adaptive multi-level split Monte Carlo scheme. Enrichment score (ES), normalized enrichment score (NES), enrichment $p$ value ($p$) and FDR-adjusted $p$ value ($p$(adj.)) were determined for each pathway.

### Pathway association with clinical variables

Associations between pathways and clinical variables were analyzed using a graph network approach. Pathways and clinical variables were represented as distinct node types in a bipartite graph, with edges denoting the degree of association. Significant pathways were identified using over-representation analysis (ORA) or gene set enrichment analysis (GSEA). The proteins linked to each significant pathway served as intermediaries to evaluate correlations with clinical variables. For each protein, two features were assessed: the correlation (ρ) with the clinical variable, and the protein's relative importance ($R$) in terms of its differential expression compared to the control group.

The clinical data included 16 features (excluding various identifiers), comprising both binary features (such as sex and ventilation interventions) and continuous features (such as age or risk scores). Additionally, features such as pathogen source, pathogen type, and comorbidities with multiple ordinal values were converted to one-hot encoded binary features. Correlation coefficients (ρ) were calculated using Pearson's correlation for continuous variables and point biserial correlation for comparisons of binary and continuous features. The relative importance $R$, inspired by the volcano plot, incorporated both impact ($\log_2$ fold change) and significance ($-\log_{10}$ adjusted $p$ value). The relative importance $R$ was calculated as the square root of the sum of the squares of impact and significance. For each statistically significant pathway, the proteins in the leading edge of the pathway were selected and their weighted correlations with a given clinical variable ($w_i = \rho_i R_i$) were summed to provide an edge weight in the bipartite graph, joining the nodes for the pathway and the clinical variable.

### Protein-protein interactions

Protein-protein interaction networks were constructed using the STRING database (version 12.0) with a minimum interaction score of 0.700 (high confidence). Differentially expressed proteins (FDR $p < 0.05$) were mapped to gene identifiers and analyzed for interactions based on experimental data, curated databases, co-expression, text-mining, and protein homology. Disease-gene associations were evaluated using the DISEASES database [32]. Differentially expressed proteins were tested for enrichment in disease categories using the hypergeometric test with Benjamini-Hochberg FDR correction. Significant associations (FDR $p < 0.05$) with $\geq 4$ genes were visualized, with bubble size indicating gene count and color reflecting significance level.

## Results

### Study population and clinical characteristics

Our final cohorts consisted of pediatric sepsis patients with age- and sex-matched healthy control subjects. The demographic details of the sepsis patients are shown in Fig. 1A. In brief, the sepsis group had a median age of 13 years (IQR 10–15) with 12 (71%) male patients. Twelve (71%) had confirmed sepsis (culture positive) while 5 (29%) were classified as suspected sepsis (culture negative). Comorbidities were present in 12 patients (71%), with 4 (24%) having multiple comorbidities. Bacterial infections were reported in 10 patients (59%), with respiratory tract infections being the most common infection site (6 patients, 35%). Chest radiograph abnormalities were documented in 12 patients (71%).

Clinical severity was substantial (Fig. 1A), with a median Glasgow Coma Scale score of 10 (IQR 6–15) and median PRISM III score of 9 (IQR 5–14). The median PIM-2 mortality risk was 9.2% (IQR 5.3%-13.2%) and median PELOD-2 score was 6 (IQR 4–7). Most patients required intensive interventions, 12 (71%) needed invasive mechanical ventilation and 13 (76%) required vasopressor support. The median PICU length of stay was 6 days (IQR 2–10) with a median total hospital stay of 15 days (IQR 9–20).

Variable associations revealed significant correlations between clinical factors (Fig. 1B, C). A strong association was observed between higher numbers of comorbidities and prolonged hospital stays, as reflected by the black color in the continuous association heatmap and the red color in the discrete significance heatmap. A significant correlation between the PIM-2 and PELOD-2 scores was observed, indicating consistency between these severity assessment tools and highlighted by the dark blue color in the continuous heatmap and the red color in the discrete heatmap.

### Sample quality assessment and data distribution

Quality control analysis identified two outlier samples within the sepsis cohort that were subsequently excluded from downstream analysis. Kernel density estimation demonstrated similar overall distribution patterns between the groups (Fig. 2A). Principal component analysis revealed distinct clustering patterns, with healthy controls forming a tight cluster while sepsis patients displayed greater heterogeneity with clear separation from the controls (Fig. 2B). The plasma proteome of children with sepsis was distinct and easily separable from the plasma proteome of healthy control subjects (Fig. 2B). A correlation heatmap with Euclidean clustering analysis confirmed stronger within-group correlations in the healthy controls than in the sepsis

A

| | |
|---|---|
| **Age (y)** | **13 (10, 15)** |
| **Sex, male** | **12 (71%)** |
| **Comorbidities** | |
| None | 5 (29%) |
| Multiple | 4 (24%) |
| Oncology | 3 (18%) |
| Neurology | 2 (12%) |
| Respiratory | 2 (12%) |
| Gastrointestinal | 1 (6%) |
| **Sepsis, proven** | **12 ( 71%)** |
| **Sepsis, suspected** | **5 (29%)** |
| **Pathogens** | |
| Gram- negative | 7 (41%) |
| Unknown | 5 (29%) |
| Gram-positive | 3 (18%) |
| Viral | 2 (12%) |
| **CXR abnormalities** | **12 (71%)** |
| **Source of pathogen** | |
| Respiratory | 6 (35%) |
| Unknown | 5 (29%) |
| Gastrointestinal | 2 (12%) |
| Infected equipment | 2 (12%) |
| Urinary tract | 1 (6%) |
| Wound | 1 (6%) |
| **PRISM 3 Score** | **9 (5, 14)** |
| **PIM-2 mortality risk (%)** | **9.2 (5.3, 13.2)** |
| **PELOD-2 Score** | **6 (4, 7)** |
| **GCS on admission** | **10 (6, 15)** |
| **Invasive ventilation** | **12 (71%)** |
| **Non-invasive ventilation** | **3 (18%)** |
| **Inotrope/ vasopressor** | **13 (76%)** |
| **PICU Days** | **6 (2, 10)** |
| **Hospital days** | **15 (9, 20)** |

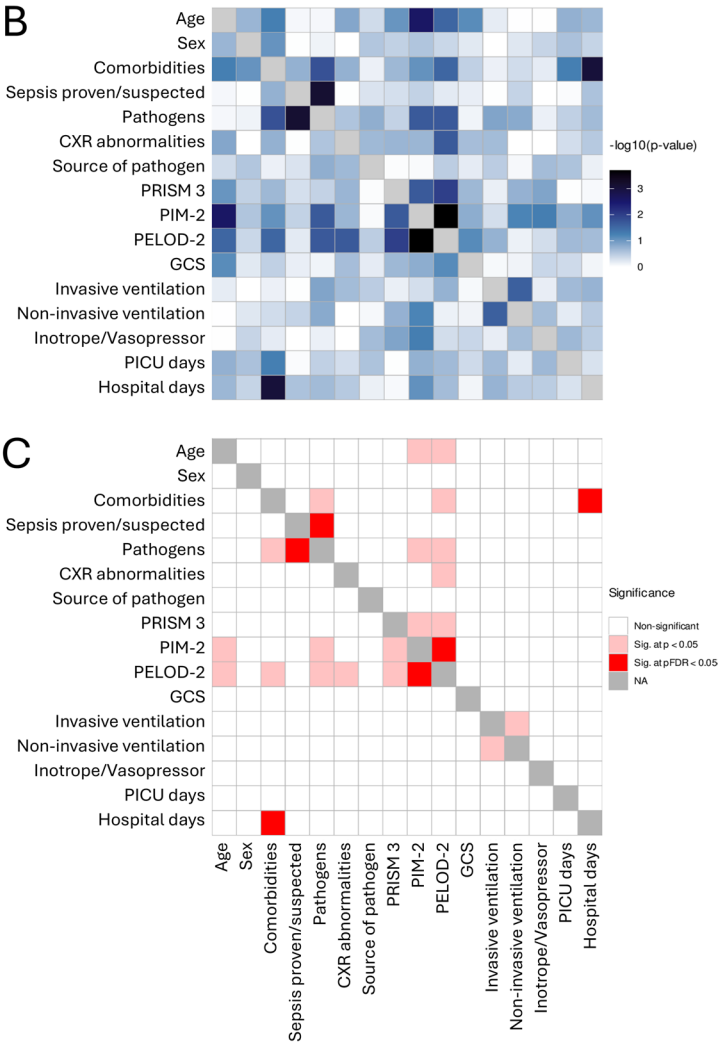


**Fig. 1** Demographic and clinical characteristics of the sepsis cohort. **A** Summary of patient demographics and biochemical parameters for pediatric sepsis patients and healthy controls, including age, sex distribution, and key clinical laboratory values. **B** Continuous association heatmap displaying pairwise correlations between all demographic and clinical variables. Association strength is represented by color intensity based on $-\log_{10}$ transformed $p$ values, ranging from white (non-significant associations) to black (highly significant associations, $p<0.001$). **C** Discrete significance heatmap showing statistical relationships between all study variables with categorical significance thresholds, where white indicates non-significant associations ($p\geq0.05$), pink indicates nominally significant associations ($p<0.05$), and red indicates associations significant after FDR correction

patients and revealed marked differences between these two groups (Fig. 2C).

## Differential protein expression analysis

Differentially expressed proteins (DEPs) in the plasma of sepsis patients relative to the plasma proteins in healthy controls are shown in a volcano plot (Fig. 3A), with positive values indicating upregulated protein levels and negative values indicating downregulated protein levels. In total, 626 plasma proteins were significantly different in sepsis and healthy controls, of which 399 were upregulated and 227 were downregulated. A heatmap of protein levels in each patient sample relative to the average across all samples is shown in Fig. 3B, indicating distinct patterns of plasma protein expression levels in sepsis patients compared to healthy controls. Figure 3C lists the 37 most differentially expressed plasma proteins in sepsis patients in rank order.

In overview, the levels of several circulating plasma proteins were higher in patients with sepsis than in healthy controls. Among the top 37 DEPs (Fig. 3C), 28 were significantly upregulated and 9 were downregulated (adjusted $p$ value$\leq0.05$) in sepsis patients. Calcitonin-related polypeptide alpha (CALCA; FC 61.406; adj. $p$ value 4.75e-21), tumor necrosis factor superfamily member 14 (TNFSF14; FC 7.994; adj. $p$ value 1.35e-15), and asialoglycoprotein

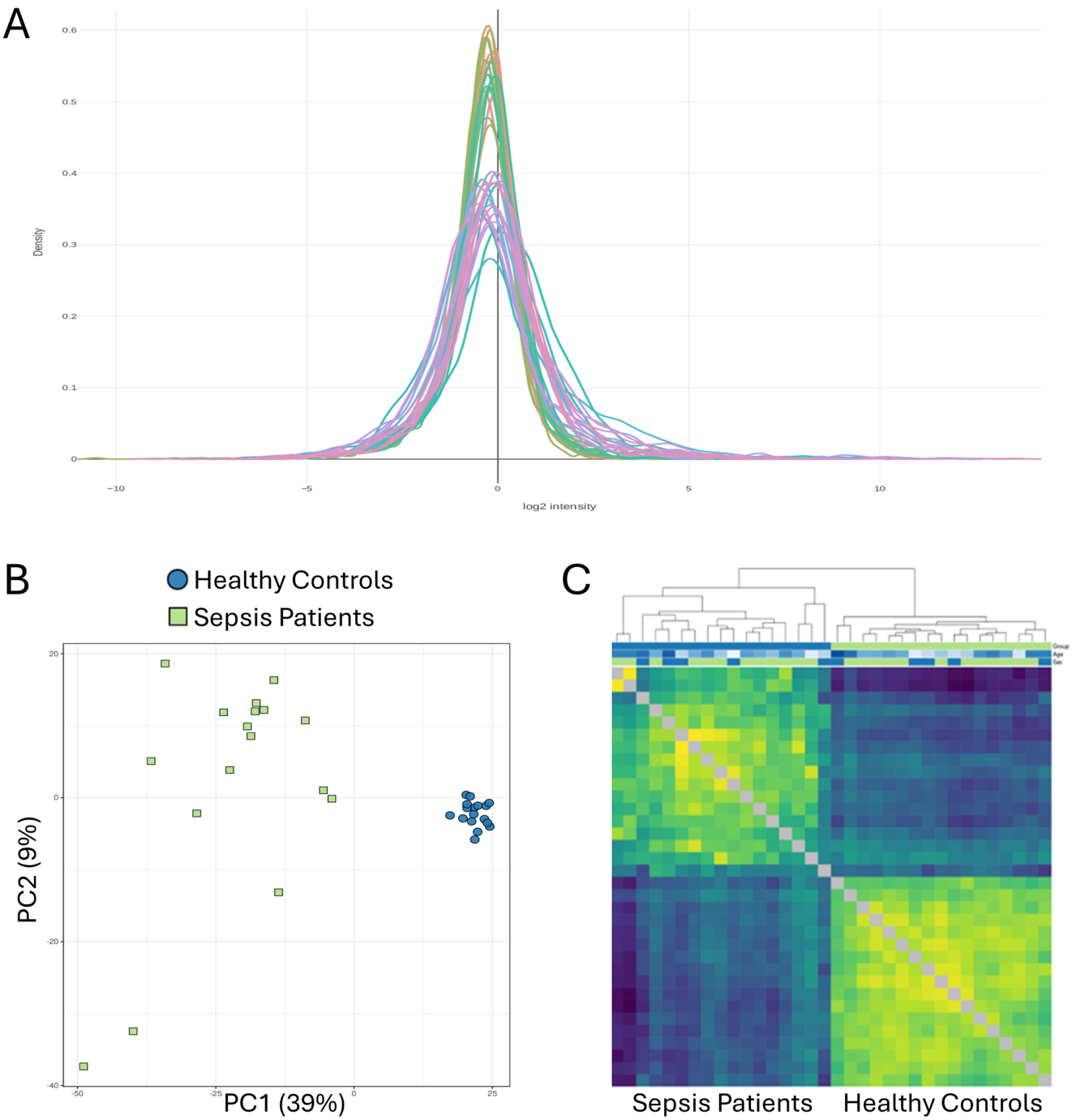


**Fig. 2** Quality control assessment and sample clustering analyses. **A** Kernel density estimates displaying the normalized protein intensity distributions for each individual sample. Overlapping distributions indicate consistent data quality and comparable dynamic ranges across samples. **B** Principal component analysis (PCA) scatter plot showing the first two principal components (PC1 and PC2) derived from the normalized proteomics dataset. Each point represents an individual patient; blue: healthy controls, green: sepsis patients. Spatial separation between groups indicates distinct proteomic profiles. **C** Hierarchical clustering heatmap displaying pairwise Pearson correlation coefficients between all samples based on normalized protein expression profiles. Samples are shown on both axes, with color intensity indicating correlation strength (yellow: high correlation, $r > 0.8$; purple: low correlation, $r < 0.5$). Dendrograms (top, left not shown) illustrate hierarchical relationships based on Euclidean distance, with sample annotations indicating clinical cohort, age, and relevant clinical variables

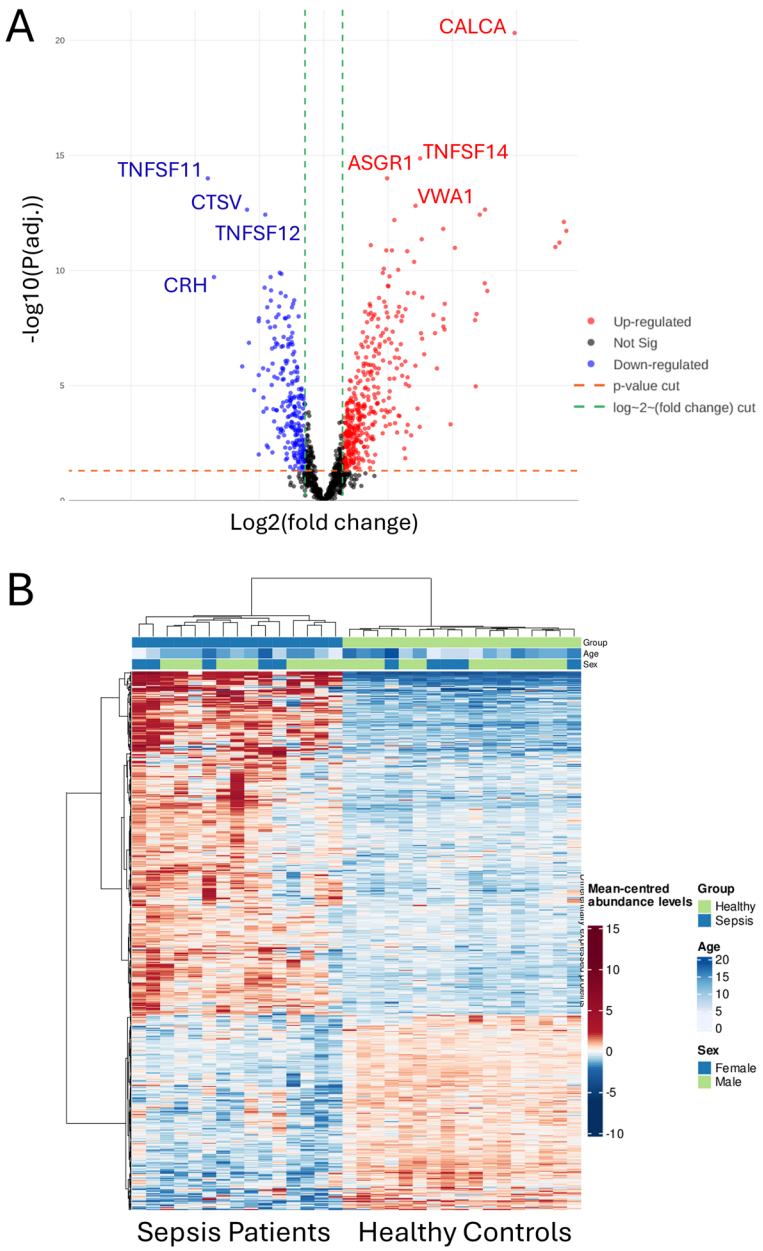


C

| Protein | FC | adj.P.Val |
|---|---|---|
| CALCA | 61.406 | 4.75E-21 |
| TNFSF14 | 7.994 | 1.35E-15 |
| TNFSF11 | -12.201 | 9.85E-15 |
| ASGR1 | 3.924 | 9.85E-15 |
| VWA1 | 7.236 | 1.53E-13 |
| CCL7 | 32.411 | 2.24E-13 |
| CTSV | -5.237 | 2.27E-13 |
| TNFSF12 | -3.532 | 3.72E-13 |
| IL1RN | 28.936 | 3.72E-13 |
| HGF | 4.581 | 6.40E-13 |
| IL6 | 177.545 | 7.69E-13 |
| TNFRSF6B | 13.147 | 1.55E-12 |
| IL6 | 187.274 | 1.88E-12 |
| CCL23 | 8.27 | 4.35E-12 |
| IL6 | 161.571 | 6.07E-12 |
| CTSL | 2.757 | 7.87E-12 |
| IL6 | 147.984 | 9.44E-12 |
| IL1RL1 | 16.918 | 1.03E-11 |
| TNFRSF10A | 4.357 | 1.33E-11 |
| TNFRSF1B | 3.852 | 1.33E-11 |
| TIMP1 | 6.047 | 1.45E-11 |
| LBP | 7.023 | 4.19E-11 |
| TNFRSF1A | 3.656 | 8.30E-11 |
| CCL2 | 4.975 | 9.25E-11 |
| DPP4 | -2.585 | 1.24E-10 |
| MCFD2 | 3.573 | 1.26E-10 |
| FKBP4 | 4.13 | 1.79E-10 |
| CRH | -10.678 | 1.91E-10 |
| HPGDS | -3.148 | 1.91E-10 |
| PLA2G2A | 32.24 | 3.56E-10 |
| IL4R | 3.978 | 4.57E-10 |
| FSTL3 | 4.04 | 4.84E-10 |
| CDON | -3.584 | 5.52E-10 |
| ADAMTS8 | -3.118 | 7.23E-10 |
| CSF3 | 34.045 | 7.71E-10 |
| NTRK2 | -2.529 | 9.42E-10 |
| VSIG4 | 7.008 | 9.42E-10 |
| WFDC2 | 6.118 | 9.42E-10 |
| GDF15 | 8.384 | 1.48E-09 |
| TNFRSF10B | 3.295 | 1.55E-09 |

**Fig. 3** Differential protein expression between pediatric patients with sepsis and healthy control subjects. **A** Volcano plot depicting significance versus magnitude of protein expression changes. The x-axis represents the log2 fold change, while the y-axis displays −log10 transformed p values. Proteins with significant differences between samples are shown in red, indicating up-regulation, or blue, indicating down-regulation. **B** Heatmap showing protein intensity per sample relative to the average level across all samples. Individual proteins are shown on the Y axis while samples are shown along the X axis. Red and blue cells correspond to higher and lower protein levels, respectively. **C** A list of the 37 plasma proteins (IL6 repeated 4 times) that were differentially expressed (adj. $p<0.05$) in sepsis patients relative to controls. Proteins upregulated in sepsis patients are shown in red and downregulated proteins are shown in blue

receptor 1 (ASGR1; FC 3.924; adj. *p* value 9.85e-15) levels were increased in sepsis patients relative to healthy controls, whereas TNF superfamily member 11 (TNFSF11; FC −12.201; adj. *p* value 9.85e-15), cathepsin V (CTSV; FC −5.237; adj. *p* value 2.27e-13), and TNF superfamily member 12 (TNFSF12; FC −3.532, adj. *p* value 3.72e-13) levels were the most significantly downregulated proteins in sepsis patients.

## Machine learning classification and feature selection

The gradient boosting classifier combined with Boruta feature selection identified 56 proteins that were optimal for distinguishing sepsis patients from healthy controls (Supplementary Fig. 1A and B). Supplementary Fig. 1A displays

the top 20 of 56 proteins ranked by their relative importance as determined by the gradient-boosting classifier and the Boruta feature selection method. Assessing all 56 proteins effectively separated the two groups into distinct clusters using t-SNE dimensionality reduction (Supplementary Fig. 1B).

Feature reduction revealed that 9 proteins, TNFRSF10A, FAP, IL-4R, CALCA, CCL3, CCL7, CTSV, RGMA, and TNFRSF1B, accounted for 90% of the total feature importance within the machine learning model used to classify patients with sepsis (Supplementary Fig. 2A and B). Supplementary Fig. 2A displays the 9 proteins ranked by their relative importance as determined by the gradient-boosting classifier and the Boruta feature selection method, which were able to separate the two groups into distinct clusters using t-SNE dimensionality reduction (Supplementary Fig. 2B). Notably, the top 3 proteins were able to provide sufficient discrimination for class separation (Supplementary Fig. 3). Supplemental Fig. 4 displays the cutoff points that enabled identification of these 9 proteins.

### Pathway enrichment analysis

ORA (over-representation analysis) identified 8 significantly enriched Reactome pathways in the plasma proteome of sepsis patients (Fig. 4A). Interleukin-10 signaling (S/N 60.00%; OR 8.99; Z-score 3.29; adj. *p* value 4.72e-06) emerged as the most significantly enriched pathway, followed by other interleukin signaling pathways and extracellular matrix (ECM) degradation. Bubble plot visualization (Fig. 4B) illustrates that most of these enriched pathways had positive Z-scores, reflecting a general trend toward upregulation of pathway components in sepsis patients. Of note, directionality (up- or down-regulation) reflects the expression patterns of individual proteins within these enriched pathways rather than coordinated pathway-level regulation. Network analysis revealed associations between enriched pathways and clinical variables (Fig. 5). "Cytokine Signaling in the Immune System" and "Immune System" pathways were identified as having the greatest number of clinical associations. Among clinical variables, the most extensive pathway associations were with gastrointestinal comorbidities, Gram-negative pathogens, and respiratory infection sources.

GSEA analysis identified 25 significantly enriched Reactome pathways (Fig. 6A). Twenty pathways were associated with over-representation of upregulated proteins, while 5 pathways exhibited over-representation of downregulated proteins. The pathways with the highest significance among upregulated protein sets included "Immune System" (NES 1.78; adj. *p* value 2.32e-09), "Signaling by Interleukins" (NES 2.01; adj. *p* value 2.87e-07), and "Cytokine Signaling in Immune System" (NES 1.85; adj. *p* value 1.10e-06). Conversely, "Axon Guidance" (NES − 1.79; adj. *p* value 0.002) and "Nervous System Development" (NES − 1.79; adj. *p* value 0.002) were the most significantly enriched pathways amongst the downregulated proteins (Fig. 6B).

As shown in Fig. 7, the GSEA-identified pathways with the greatest clinical variable associations were GPCR-associated pathways (ligand binding and signaling) and interleukin signaling pathways. Associations between multiple GSEA pathways and Gram-negative pathogen infections were also evident.

### Network analysis

STRING protein-protein interaction network analysis revealed that the differentially expressed proteins in the plasma of sepsis patients formed highly interconnected functional networks with significant interactions (Fig. 8A). Several proteins emerged as highly connected network hubs, including IL-6, CRP, IFNG, IL-10, CXCL8, and CXCL10. Disease association enrichment analysis demonstrated significant associations between these network hubs and clinically relevant disease categories (Fig. 8B). The most significant associations were with respiratory diseases including coronavirus infectious disease, COVID-19, respiratory failure, pneumonia, and ARDS. Additional associations included leukopenia and lymphopenia (Fig. 8B).

## Discussion

This exploratory case-control cohort study utilized high-throughput proteomic profiling to characterize the molecular landscape of pediatric sepsis and resulted in the identification of 626 differentially expressed plasma proteins in patients with sepsis. Machine learning demonstrated that a minimal set of 9 protein biomarkers were able to distinguish sepsis patients from healthy controls, while pathway-level analysis provided novel insights into the complex, network-driven pathophysiology of pediatric sepsis. Our pathway enrichment analyses demonstrated that pediatric sepsis is characterized by dysregulation of multiple biological networks, the most notable being interleukin signaling pathways (IL-10, IL-4, IL-13), neutrophil degranulation, ECM degradation, and metabolic reprogramming. Network analyses revealed distinct patterns of pathway activation, and that the degree of immune pathway dysregulation was associated with organ dysfunction severity.

The clinical characteristics of our pediatric sepsis cohort align with previously published literature [33, 34]. The predominance of bacterial infections and respiratory tract involvement reflects established epidemiological patterns in

A

| Description | S/N (%) | OR | Z-score | P (adj.) |
|---|---|---|---|---|
| Interleukin-10 signaling | 60.00 | 8.99 | 3.29 | 4.72E-06 |
| Activation of Matrix Metalloproteinases | 71.43 | 14.39 | 1.60 | 4.47E-04 |
| Degradation of the extracellular matrix | 45.95 | 5.02 | 1.48 | 6.35E-04 |
| Signaling by Interleukins | 28.47 | 2.50 | 2.99 | 0.002 |
| Cytokine Signaling in Immune system | 25.40 | 2.17 | 2.91 | 0.003 |
| Collagen degradation | 55.56 | 7.17 | 2.36 | 0.004 |
| Interleukin-4 and Interleukin-13 signaling | 37.78 | 3.56 | 2.53 | 0.006 |
| Immune System | 19.91 | 1.69 | 3.37 | 0.030 |

B

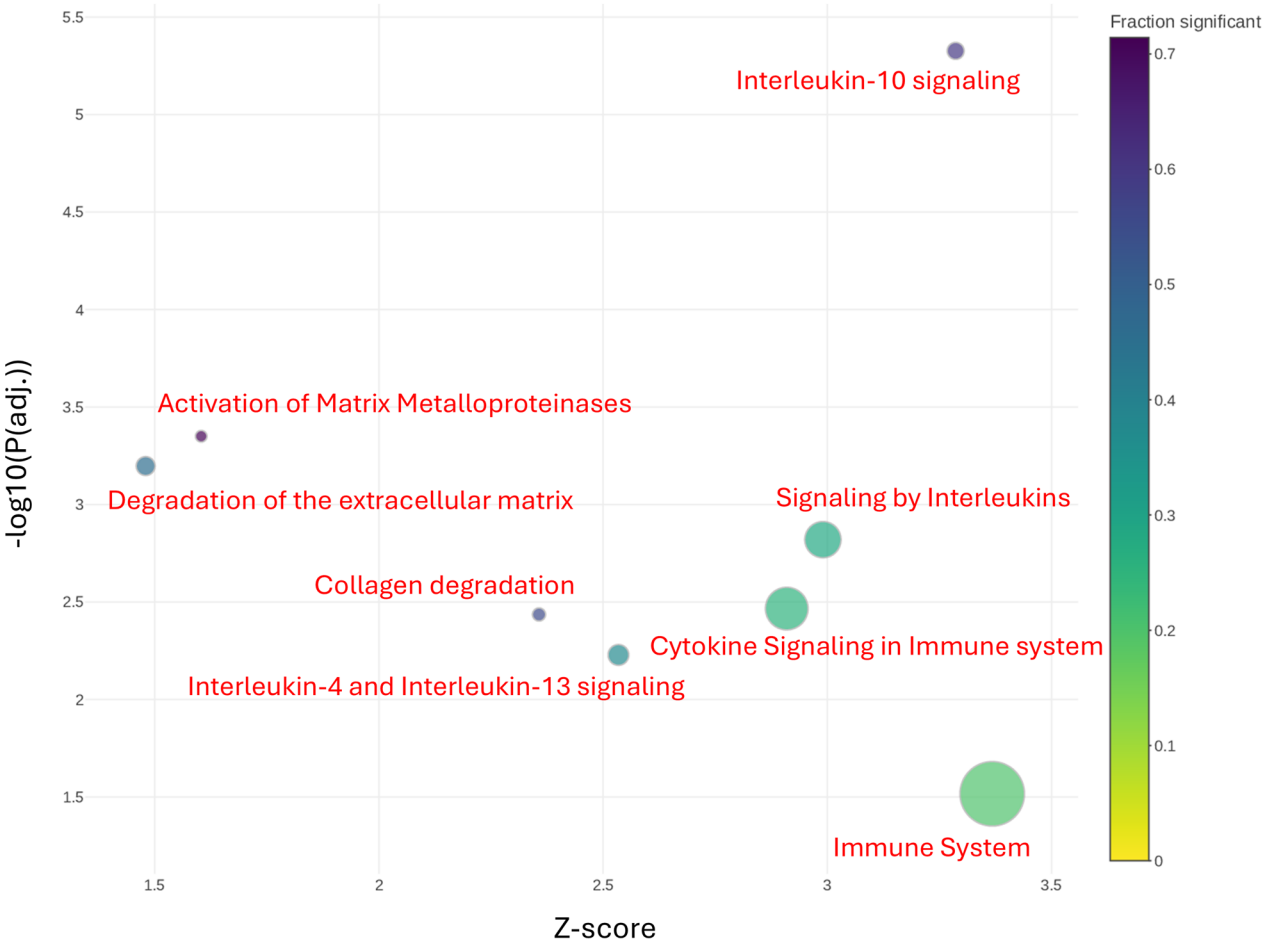


**Fig. 4** Functional enrichment using over-representation analysis (ORA). **A** Table of significantly enriched Reactome pathways identified by over-representation analysis comparing sepsis patients to healthy controls. Pathways are ranked by adjusted $p$ value (FDR $p<0.05$). Additional columns display the number of differentially expressed proteins mapping to each pathway, total pathway size, enrichment ratio, and combined enrichment score. **B** Bubble plot visualizing pathway enrichment results. The y-axis represents statistical significance as $-\log_{10}$ (adjusted $p$ value), and the x-axis shows the directional enrichment z-score. Positive z-scores indicate predominant upregulation; negative z-scores indicate predominant downregulation. Bubble size is proportional to pathway size (total number of proteins), and bubble color represents the fraction of proteins within the pathway that are differentially expressed

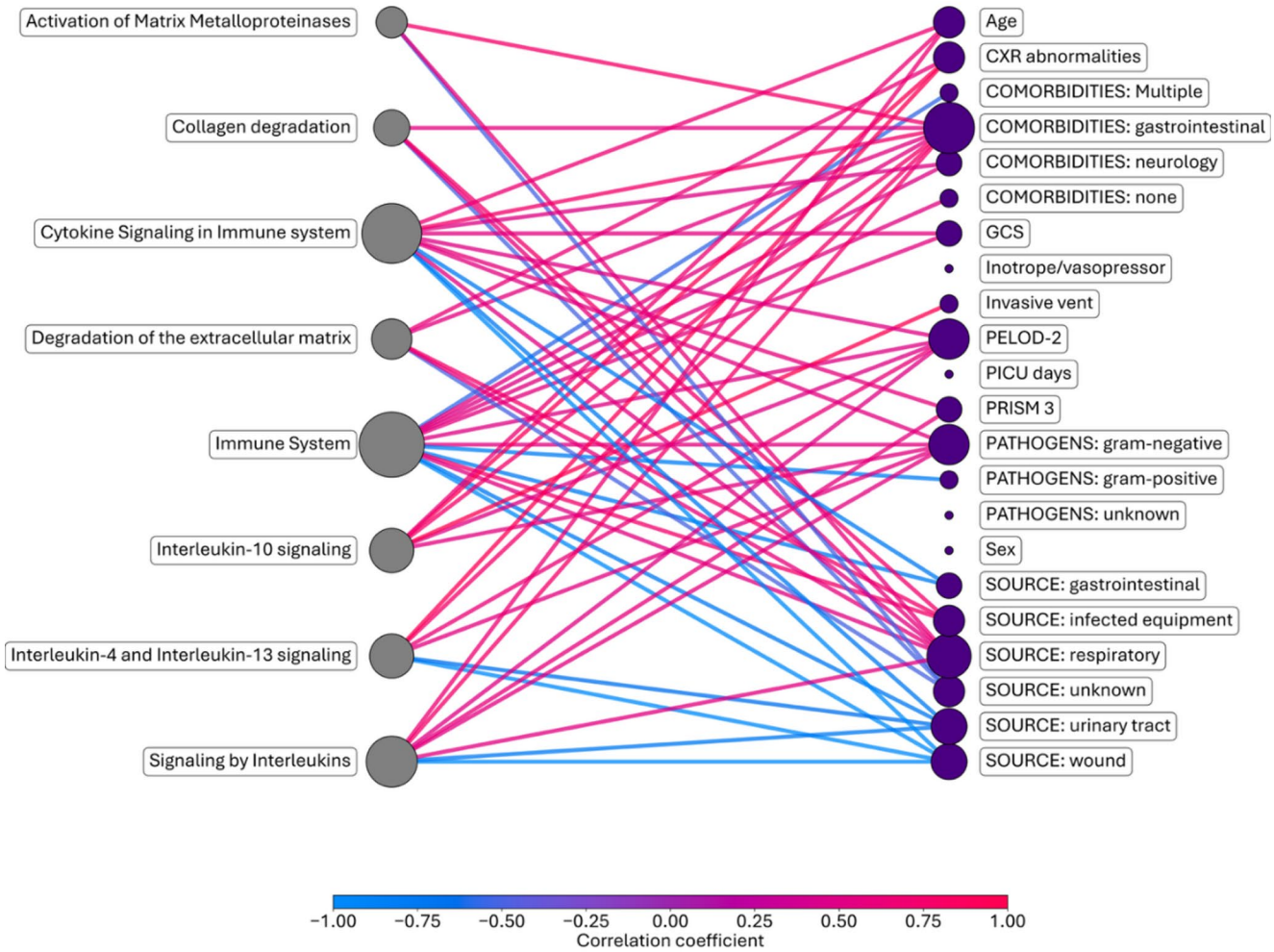


**Fig. 5** Network visualization of pathway-clinical variable associations from over-representation analysis. Network diagram illustrating significant correlations between enriched Reactome pathways (identified by ORA) and clinical/demographic variables. Pathways and clinical variables are represented as nodes, with node size proportional to the number of significant connections. Edges represent significant correlations, with edge color indicating correlation direction and magnitude: red for positive correlations, blue for negative correlations (color intensity reflects correlation strength). Only correlations with $r \geq 0.5$ and $p < 0.05$ are displayed to enhance interpretability

pediatric sepsis. The high prevalence of comorbidities and the substantial requirement for intensive interventions, such as mechanical ventilation and vasopressor support, underscore the severity of illness in our cohort and are consistent with mortality risk factors identified in larger pediatric sepsis studies. The median age of 13 years in our cohort was higher than what is typically reported in pediatric sepsis literature [35, 36], possibly reflecting referral patterns to our tertiary care center or seasonal variation in sepsis epidemiology.

The 626 dysregulated plasma proteins identified by PEA analysis included 399 upregulated and 227 downregulated proteins. Proinflammatory mediators involved in immune system activation, including CALCA, TNFSF14, and ASGR1, were among the most overexpressed proteins. CALCA was a notable finding, given its established role in systemic inflammation and sepsis. CALCA encodes calcitonin (and its precursor, procalcitonin [PCT]) and CGRP through tissue-specific alternative splicing. While PCT levels were associated with sepsis severity and are widely used as a clinical biomarker, the role of CGRP is less clearly defined. CGRP is a vasoactive neuropeptide that promotes the release of proinflammatory cytokines and supports a Th17-mediated immune response [37]. In addition, we identified TNFSF14, a key activator of both innate and adaptive immune responses [38], and ASGR1, the major subunit of the asialoglycoprotein receptor (ASGR) that contributes to immune regulation by clearing desialylated glycoproteins from circulation, removing apoptotic cells, activating lymphocytes, and promoting additional inflammatory processes [39]. Finally, IL6, a classic proinflammatory cytokine and endogenous pyrogen, was upregulated in the plasma of sepsis patients. While IL6 upregulation is not specific to sepsis, it is commonly associated with infection

A

| Description | Size | NES | P (adj.) |
|---|---|---|---|
| Immune System | 432 | 1.78 | 2.32E-09 |
| Signaling by Interleukins | 137 | 2.01 | 2.87E-07 |
| Cytokine Signaling in Immune system | 189 | 1.85 | 1.10E-06 |
| Innate Immune System | 211 | 1.70 | 1.32E-04 |
| Interleukin-10 signaling | 30 | 1.98 | 3.11E-04 |
| Interleukin-4 and Interleukin-13 signaling | 45 | 1.87 | 0.001 |
| Cellular responses to stress | 75 | 1.77 | 0.001 |
| Cellular responses to stimuli | 75 | 1.77 | 0.001 |
| Axon guidance | 73 | -1.79 | 0.002 |
| Nervous system development | 73 | -1.79 | 0.002 |
| GPCR ligand binding | 59 | 1.78 | 0.004 |
| Neutrophil degranulation | 120 | 1.65 | 0.004 |
| Peptide ligand-binding receptors | 43 | 1.77 | 0.004 |
| L1CAM interactions | 18 | -1.98 | 0.006 |
| Class A/1 (Rhodopsin-like receptors) | 46 | 1.71 | 0.012 |
| Chemokine receptors bind chemokines | 29 | 1.74 | 0.013 |
| Metabolism of RNA | 17 | 1.73 | 0.021 |
| Developmental Biology | 143 | -1.42 | 0.028 |
| HIV Infection | 16 | 1.68 | 0.028 |
| Asparagine N-linked glycosylation | 28 | 1.66 | 0.031 |
| Cell Cycle | 35 | 1.65 | 0.036 |
| Regulation of IGF transport and uptake by IGFBPs | 44 | 1.58 | 0.043 |
| PI3K/AKT Signaling in Cancer | 39 | -1.64 | 0.044 |
| M Phase | 17 | 1.64 | 0.044 |
| Signaling by GPCR | 77 | 1.52 | 0.044 |

B

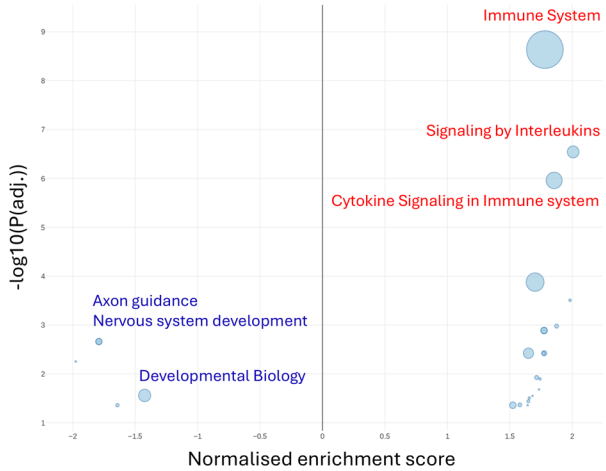


**Fig. 6** Functional enrichment analysis using Gene Set Enrichment Analysis (GSEA). **A** Table of significantly enriched Reactome pathways identified by gene set enrichment analysis comparing the ranked protein expression profiles of sepsis patients versus healthy controls. Pathways are ranked by normalized enrichment score (NES), with FDR $p<0.05$ considered significant. Additional columns include normalized enrichment score (NES), FDR-adjusted $p$ value, leading edge size (number of core enrichment proteins), and enrichment direction (upregulated: red; downregulated: blue). **B** Bubble plot displaying GSEA enrichment results. The y-axis represents $-\log_{10}$ (adjusted $p$ value), and the x-axis shows the directional enrichment z-score. Positive z-scores indicate pathways enriched in upregulated proteins; negative z-scores indicate pathways enriched in downregulated proteins. Bubble size corresponds to total pathway size

and inflammation, making it a confirmatory, albeit nonspecific, biomarker in the context of sepsis [40].

Several of the plasma proteins that were reduced in sepsis patients compared to healthy controls, such as TNFSF11, TNFSF12, and CTSV, also have established roles in immune responses. TNFSF11 is a type II transmembrane protein that attenuates macrophage proinflammatory responses [41] and TNFSF12, which plays a key regulatory role in both inflammation and cell death, has been previously reported to be depleted in sepsis [42]. CTSV has been associated with increased production of IL-6, tumor necrosis factor (TNF), and C-X-C motif chemokine ligand 15 (CXCL15), consistent with multiple roles in the inflammatory response. The implications of CTSV downregulation in sepsis are currently unclear. Possibilities include immune system dysregulation and impaired cellular migration, consistent with its established roles in elastin degradation [43].

Machine learning identified 56 plasma proteins that could be used to clearly separate sepsis patients from healthy controls. Notably, only nine of these proteins, TNFRSF10A, FAP, IL-4R, CALCA, CCL3, CCL7, CTSV, RGMA, and TNFRSF1B, were sufficient to account for 90% of the total feature importance and were sufficient to distinguish between these two groups. TNF receptor superfamily member 10 A (TNFRSF10A) is a cell surface receptor involved in apoptosis, inflammation, and necrosis. TNFRSF10A binds TNF-related apoptosis-inducing ligand (TRAIL) to activate NF-κB inflammatory and death receptor signaling pathways [44]. Fibroblast activation protein (FAP) is a serine protease expressed by activated fibroblasts during inflammation. FAP has a wide range of substrates, including lysyl oxidase-like 1 (LOXL1), CXCL5, colony-stimulating factor 1 (CSF-1), and C1q and TNF related 6 (C1QTNF6), consistent with central roles in inflammation, ECM remodeling, and fibrinolysis [45, 46]. Interleukin-4 receptor (IL-4R) binds interleukin-4 (IL-4), a cytokine with a significant regulatory role in the inflammatory response [47]. Chemokine ligand 3 (CCL3) recruits immune cells and is previously reported to be elevated during sepsis [48]. Chemokine ligand 7 (CCL7) attracts monocytes, eosinophils, basophils, dendritic cells, NK cells, and activated T lymphocytes [49]. Repulsive guidance molecule A (RGMA), expressed in leukocytes and epithelial cells, inhibits leukocyte migration and dampens inflammatory responses [50] and may contribute to the altered immune regulation observed in sepsis. TNF receptor superfamily member 1B (TNFRSF1B) is involved in NF-κB and IL-6 signaling and activates lymphokine-activated killer cells and NK cells. It also regulates cellular proliferation, apoptosis, and cytotoxicity. In sepsis, elevated levels of its soluble form may act as a buffer against excessive cytokine responses [51].

Our pathway enrichment analyses revealed the dysregulation of immune and inflammatory networks extending beyond isolated biomarker abnormalities. Both ORA and GSEA converged on interleukin signaling as a central node of dysregulation, with IL-10 signaling emerging as the most significantly enriched pathway. IL-10 functions primarily by inhibiting proinflammatory cytokine production in myeloid cells, NK cells, and T lymphocytes, with expression levels correlating with inflammatory response

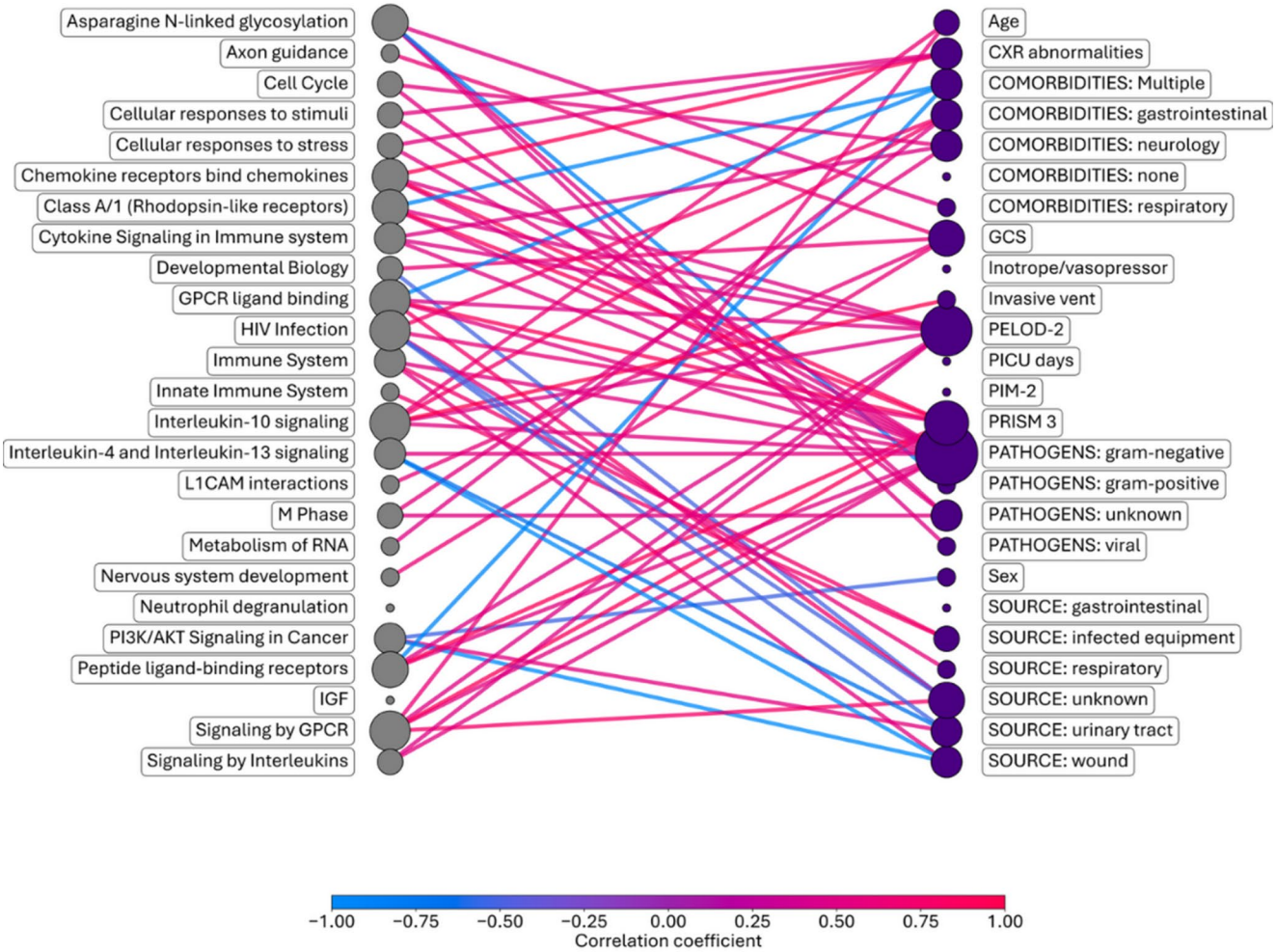


**Fig. 7** Network visualization of pathway-clinical variable associations from Gene Set Enrichment Analysis. Network diagram displaying significant correlations between enriched Reactome pathways (identified by GSEA) and clinical/demographic variables measured in the study cohort. Nodes represent either pathways or clinical variables, with node size proportional to connectivity (number of significant edges). Edges indicate significant correlations between pathway enrichment scores and clinical parameters, colored by correlation direction: red for positive correlations, blue for negative correlations (color saturation reflects correlation magnitude). Only associations with $r \geq 0.5$ and $p < 0.05$ are visualized to highlight the most robust pathway-phenotype relationships

intensity [52, 53]. This finding highlights the delicate balance between hyperinflammation and compensatory immunosuppression characteristic of sepsis. The enrichment of IL-4 and IL-13 signaling pathways further illustrates this immunological reprogramming. These interleukins promote Th2 polarization, drive macrophage differentiation toward anti-inflammatory M2 phenotypes, suppress Th1-mediated proinflammatory responses, and enhance expression of IL-1 receptor antagonist and IL-1 receptor type II [47]. Their upregulation is consistent with a systemic shift toward immunosuppression that may render patients vulnerable to secondary infections.

GSEA uniquely identified significant enrichment of neutrophil degranulation pathways, indicating dysregulated innate immune cell function. While neutrophil degranulation aids pathogen clearance, overactivation causes tissue damage through release of proteolytic enzymes and inflammatory cytokines. Neutrophil extracellular traps (NETs) composed of DNA and antimicrobial proteins are abundantly released during sepsis and contribute to endothelial dysfunction and organ failure in sepsis [52, 53]. The concurrent downregulation of PI3K/Akt signaling provides mechanistic insight into neutrophil dysfunction, as this pathway is essential for oxidative burst and phagocytic capacity. Murine sepsis models demonstrate that PI3K inhibition markedly impairs neutrophil antimicrobial functions, consistent with pathway suppression and functional exhaustion of these cells, despite the quantitative neutrophilia seen in sepsis [52, 53].

Dysregulation of the growth hormone/insulin-like growth factor (GH/IGF) axis identified through GSEA suggests the possibility of metabolic reprogramming during

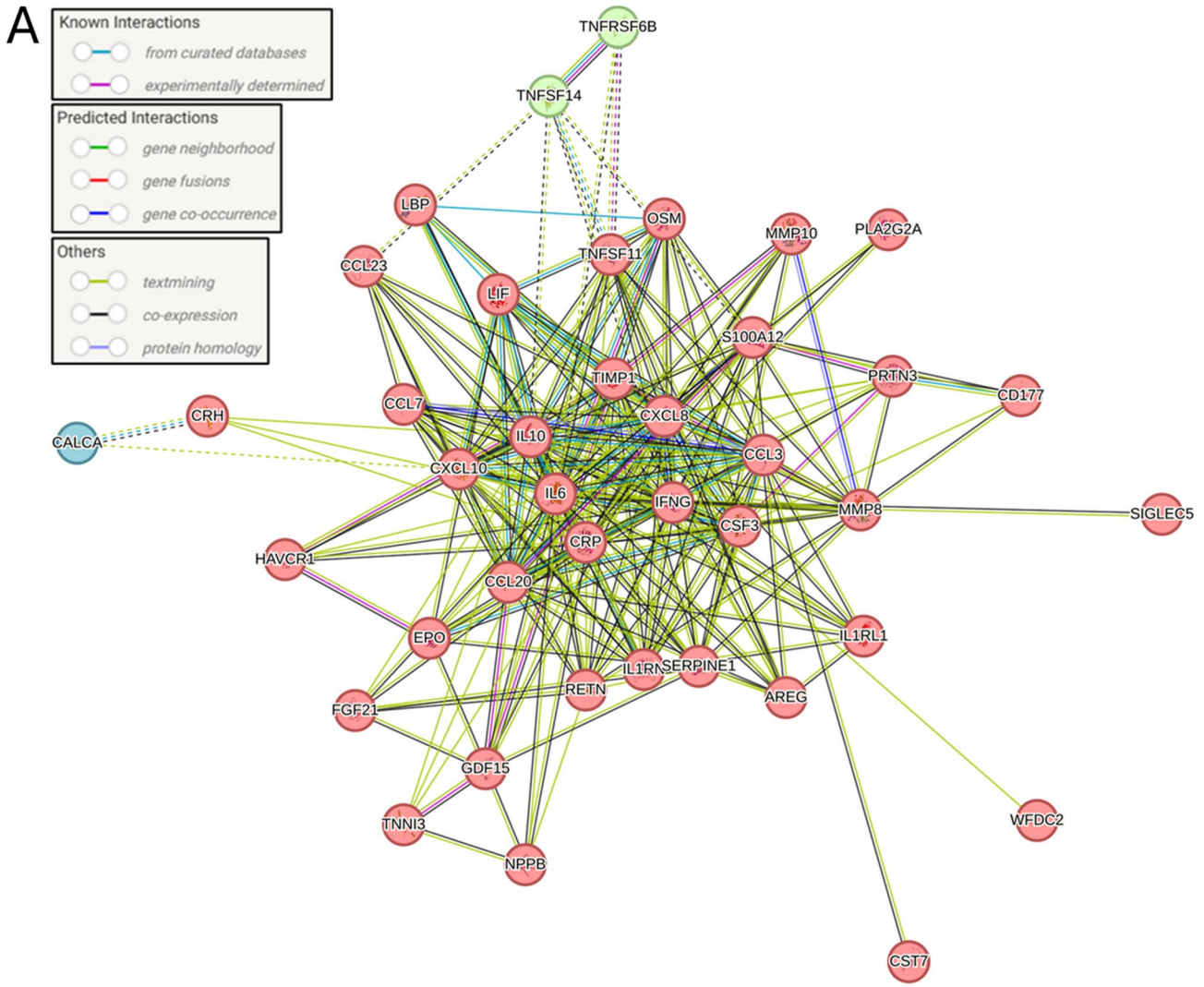
A
Known Interactions
from curated databases
experimentally determined
Predicted Interactions
gene neighborhood
gene fusions
gene co-occurrence
Others
textmining
co-expression
protein homology
TNFRSF6B
TNFSF14
LBP
OSM
MMP10
PLA2G2A
CCL23
TNFSF11
LIF
S100A12
PRTN3
CD177
TIMP1
CCL7
CXCL8
CRH
CALCA
IL10
CCL3
CXCL10
IL6
IFNG
MMP8
SIGLEC5
CSF3
CRP
HAVCR1
CCL20
EPO
IL1RL1
IL1RN
SERPINE1
RETN
AREG
FGF21
GDF15
TNNI3
WFDC2
NPPB
CST7

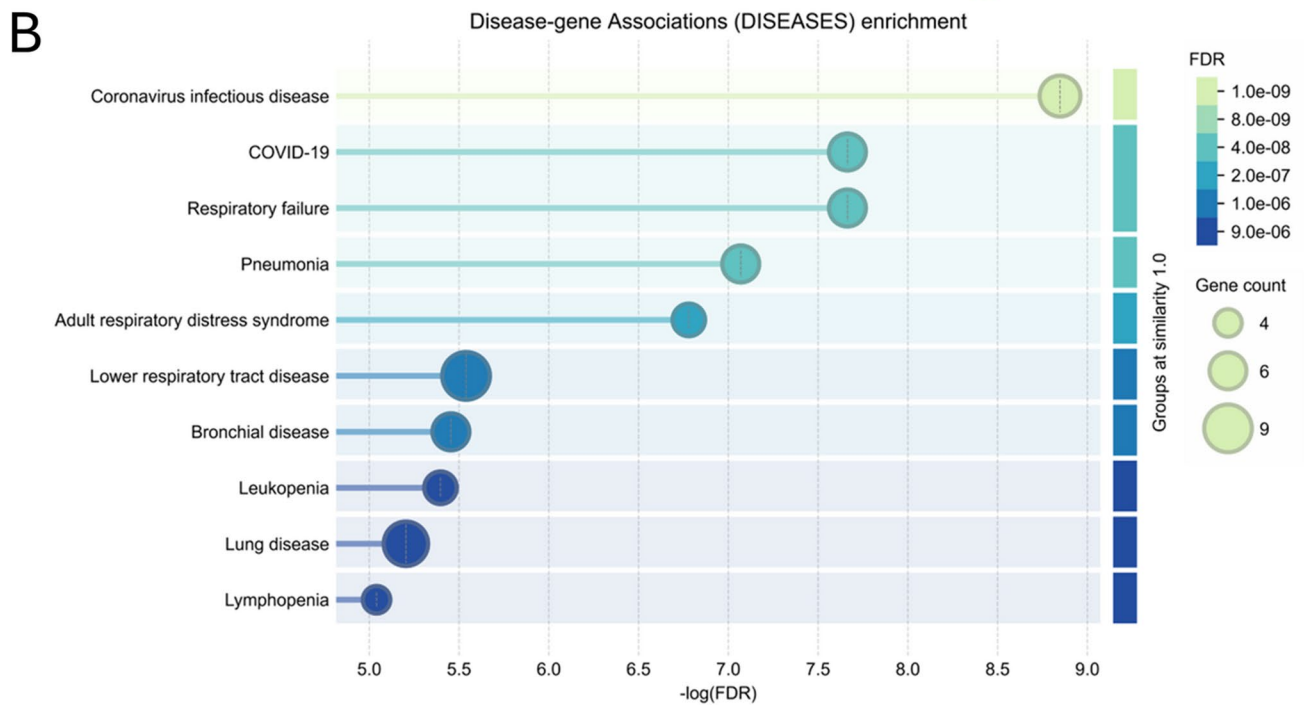
B
Disease-gene Associations (DISEASES) enrichment
Coronavirus infectious disease
COVID-19
Respiratory failure
Pneumonia
Adult respiratory distress syndrome
Lower respiratory tract disease
Bronchial disease
Leukopenia
Lung disease
Lymphopenia
5.0
5.5
6.0
6.5
7.0
7.5
8.0
8.5
9.0
-log(FDR)
Groups at similarity 1.0
FDR
1.0e-09
8.0e-09
4.0e-08
2.0e-07
1.0e-06
9.0e-06
Gene count
4
6
9

**Fig. 8** Protein-protein interaction network and disease association analysis. **A** STRING database protein-protein interaction network of differentially expressed proteins in pediatric sepsis. Nodes represent individual proteins (gene symbols shown). Edge colors indicate evidence type: cyan (curated databases), magenta (experimental), green (gene neighborhood), red (gene fusions), blue (co-occurrence), yellow (text-mining), black (co-expression), purple (protein homology). Line thickness reflects interaction confidence score. Minimum interaction score: 0.700 (high confidence). **B** Disease-gene association enrichment from DISEASES database. X-axis shows $-\log_{10}$(FDR), bubble size indicates gene count (4–9 genes), and color represents significance level (light green: FDR ~ $10^{-9}$; dark blue: FDR ~ $10^{-6}$)

critical illness. Sepsis disrupts this axis through reduced pulsatile GH secretion and increased GH resistance, evident as decreases in IGF-1 and IGF binding protein − 3 (IGFBP-3) that are concurrent with increases in IGFBPs-1, -2, and − 6. Elevated levels of proinflammatory cytokines such as TNF, IL-1, and IL-6 drive catabolic processes including lipolysis and proteolysis [52, 53]. This endocrine dysregulation contributes to muscle wasting, impaired wound healing, and prolonged recovery, underscoring the inextricable link between metabolic and immunological dysfunction in pediatric sepsis.

ORA identified significant enrichment of ECM degradation pathways, potentially a reflection of widespread tissue damage. Excessive activation of matrix metalloproteinases (MMPs), a disintegrin and metalloproteinase with thrombospondin motifs (ADAMTS), and other matrix-associated enzymes can result in ECM breakdown, barrier dysfunction, and microvascular leak. Elevated collagen fragments detected in blood and bronchoalveolar lavage fluid of sepsis patients may serve as biomarkers of ongoing tissue injury, while reduced collagen synthesis contributes to impaired repair [54–56]. ECM fragments also function as damage-associated molecular patterns that perpetuate inflammation, creating a cycle of tissue damage and immune activation.

An unexpected finding from GSEA was the downregulation of neural guidance pathways, including axon guidance and L1 cell adhesion molecule (L1CAM) signaling. While traditionally associated with nervous system development, neural guidance molecules like netrin-1 are increasingly being recognized as immunomodulators. While netrin-1 normally limits neutrophil infiltration and promotes inflammatory resolution, its suppression during bacterial infection facilitates increased neutrophil recruitment [44]. L1CAM pathway activation normally promotes cell migration and tissue invasion, and while downregulation could be interpreted to suggest disruption of leukocyte trafficking and endothelial barrier function, the roles of this pathway in acute inflammation remain poorly characterized and in need of further investigation [55, 56].

Network analyses linking enriched pathways to clinical variables (Figs. 5 and 7) indicated that specific pathogen types and infection sources triggered distinct patterns of biological pathway activation, rather than uniform immune responses. ORA analysis identified extensive clinical associations with cytokine signaling and other immune system pathways, while GSEA identified GPCR-associated pathways and interleukin signaling as highly connected network hubs. Importantly, immune system pathways were consistently associated with illness severity metrics, particularly PELOD-2 scores, suggesting that the degree of pathway dysregulation is associated with organ dysfunction severity, with potential to serve as biological readouts of disease progression [57]. Notably, Gram-negative bacterial infections were associated with multiple pathways in both ORA and GSEA analyses, possibly reflecting the potent immunostimulatory properties of lipopolysaccharides that drive widespread NF-κB activation and cytokine production [58]. Similarly, extensive pathway connections with respiratory tract infections were observed, potentially reflecting the unique immunological environment of the lung and its large capillary surface area that can facilitate the dissemination of systemic inflammatory mediators [59]. Additionally, gastrointestinal comorbidities emerged as strongly associated with pathway dysregulation, consistent with the hypothesis that underlying gut pathology may prime or modify systemic immune responses during sepsis [60]. Collectively, these pathogen- and site-specific associations suggest that pediatric sepsis encompasses distinct endotypes with different underlying biological mechanisms, supporting the potential for pathway-based patient stratification and precision therapeutic targeting [61].

Protein-protein interaction network analysis using the STRING database revealed that differentially expressed proteins in pediatric sepsis form highly interconnected functional networks, with 86% of proteins showing at least one significant interaction. This extensive connectivity indicates that sepsis-induced proteomic changes reflect dysregulation of biological networks rather than isolated molecular events [62]. Several proteins, including IL6, CRP, IFNG, IL-10, CXCL8, and CXCL10, emerged as highly connected hubs with more than 15 interactions each, suggesting that these molecules serve as central regulatory nodes in the sepsis response. The identification of hub proteins is particularly valuable for therapeutic development, as these highly connected nodes may represent leverage points where targeted interventions could produce cascade effects throughout the network [63]. Disease association enrichment analysis demonstrated that this differentially expressed protein signature had significant overlap with known disease-associated gene sets, validating the clinical relevance of our findings. The strongest disease association enrichment was with respiratory diseases, including coronavirus infectious disease, COVID-19, respiratory failure, pneumonia, and acute respiratory distress syndrome [64]. The prominent COVID-19

association is particularly noteworthy given that our cohort consisted primarily of bacterial sepsis cases without SARS-CoV-2 infection. This unexpected convergence suggests that severe bacterial sepsis and severe viral infections activate overlapping host response pathways, indicating that fundamental mechanisms of critical illness may be conserved across different infectious etiologies [65, 66]. Additional disease association enrichment for leukopenia and lymphopenia reflected the systemic immune dysfunction characteristic of sepsis, further validating that our proteomic signature captures clinically relevant pathophysiology [62]. These network and disease association analyses provide complementary perspectives, with interaction networks revealing how proteins might function together mechanistically, while disease associations confirm that these molecular patterns correspond to recognizable clinical syndromes.

Our study has several important methodological limitations that must be considered when interpreting our findings. First, this single-center exploratory study assessed a relatively small sample size, and our findings will require validation in larger, independent cohorts. Given the limited sample size, the protein signature identified in this study should be viewed as a set of prioritized candidates for future investigation rather than a definitive diagnostic tool, and the results should be interpreted as exploratory indicators of pathway-level changes rather than conclusive evidence of activation. Second, our cohort's median age of 13 years is substantially higher than typical pediatric sepsis populations, limiting generalizability to younger children who may exhibit distinct immune responses. Third, samples were assessed at a single timepoint, preventing us from capturing temporal evolution of sepsis pathophysiology or distinguishing disease severity from outcome prediction. Fourth, our limited sample size prevented stratification by disease severity, pathogen type, or infection source, and we did not examine associations with key clinical outcomes such as mortality, organ dysfunction, or ventilator duration. Fifth, our lack of sepsis mimic controls prevented us from distinguishing between sepsis-specific and generic critical illness responses. Furthermore, investigating additional sepsis etiologies and causative organisms would help to better delineate disease pathobiology. Despite these limitations, we maintain that this study provides robust exploratory systems-level insights into pediatric sepsis pathophysiology.

## Conclusions

This exploratory proteomic study identified 626 differentially expressed proteins in pediatric sepsis and demonstrated that pathway enrichment analyses can provide novel biological insights that traditional single-biomarker analyses cannot. While machine learning identified a minimal 9-protein signature distinguishing sepsis from health, pathway-level analysis highlighted additional complexity of sepsis pathophysiology including the dysregulation of interleukin signaling networks (notably IL-10, IL-4, and IL-13), neutrophil degranulation, growth hormone axis disruption, ECM degradation, and neural guidance pathways. Network analyses demonstrated correlations between immune pathway dysregulation and organ dysfunction severity (PELOD-2 scores). Protein-protein interaction analysis identified highly connected hub proteins, IL-6, IL-10, CXCL8, CXCL10, as central regulatory nodes, while disease association enrichment revealed convergent host response pathways across different infectious etiologies. These findings suggest that pathway-based biomarker analyses may provide biological readouts of disease progression and enable endotype-specific patient stratification superior to conventional severity scores or individual protein biomarkers. However, validation in larger, multicenter cohorts with longitudinal sampling and outcome-focused endpoints will be required to translate these pathway-level insights into clinically actionable tools for risk stratification and precision immunomodulatory therapy in pediatric sepsis.

**Supplementary Information** The online version contains supplementary material available at https://doi.org/10.1007/s00011-026-02200-1.

**Acknowledgements** Not applicable.

**Author contributions** DDF conceived and designed the study. VS, LVN, EC and DDF collected human samples and clinical data. VS, LVN, DT, MD and DDF analyzed all data and produced Figures. VS, LVN, MM, DBO, GC and DDF wrote the manuscript with input from all other authors.

**Funding** DDF received study funding from the GSK Chair in Clinical Pharmacology (Western University), the London Health Sciences Foundation (https://lhsf.ca/), the London Community Foundation and the AMOSO Innovation Fund.

**Data availability** The datasets generated and/or analyzed during the current study are available from the corresponding author upon reasonable request.

## Declarations

**Conflict of interest** The authors declare no competing interests.

**Ethics approval and consent to participate** This study was approved by the Western University, Human Research Ethics Board (REB #s 6970; #100036; # 6963). Our experimental methods are performed in accordance with ethical standards of the responsible committee on human experimentation with the Helsinki Declaration of 1975. Informed written consent was obtained from either participants or their legal guardians.

**Consent for publication** Not applicable.

## References

1. Weiss SL, Fitzgerald JC. Pediatric sepsis diagnosis, management, and sub-phenotypes. Pediatrics 2024;153(1).
2. Sanchez-Pinto LN, Bennett TD, DeWitt PE, Russell S, Rebull MN, Martin B, Akech S, Albers DJ, Alpern ER, Balamuth F, et al. Development and validation of the phoenix criteria for pediatric sepsis and septic shock. JAMA. 2024;331(8):675–86.
3. Weiss SL, Peters MJ, Alhazzani W, Agus MSD, Flori HR, Inwald DP, Nadel S, Schlapbach LJ, Tasker RC, Argent AC, et al. Surviving sepsis campaign international guidelines for the management of septic shock and sepsis-associated organ dysfunction in children. Pediatr Crit Care Med. 2020;21(2):e52–106.
4. van der Poll T, van de Veerdonk FL, Scicluna BP, Netea MG. The immunopathology of sepsis and potential therapeutic targets. Nat Rev Immunol. 2017;17(7):407–20.
5. Yang Z, Gao Y, Zhao L, Lv X, Du Y. Molecular mechanisms of Sepsis attacking the immune system and solid organs. Front Med. 2024;11:1429370.
6. Barichello T, Generoso JS, Singer M, Dal-Pizzol F. Biomarkers for sepsis: more than just fever and leukocytosis-a narrative review. Crit Care. 2022;26(1):14.
7. Feng Z, Wang L, Yang J, Li T, Liao X, Kang Y, Xiao F, Zhang W. Sepsis: the evolution of molecular pathogenesis concepts and clinical management. MedComm. 2025;6(3):e70109.
8. Lim PPC, Bondarev DJ, Edwards AM, Hoyen CM, Macias CG. The evolving value of older biomarkers in the clinical diagnosis of pediatric sepsis. Pediatr Res. 2023;93(4):789–96.
9. Van Nynatten LR, Bokhary D, Wong MYS, Wang J, Fero H, McChesney C, Fiorini K, Blake L, Fraser DD, Slessarev M, et al. Predictive enrichment using biomarkers in studies of critically-ill patients with sepsis: a systematic review. Crit Care. 2025;29(1):504.
10. Leonard S, Guertin H, Odoardi N, Miller MR, Patel MA, Daley M, Cepinskas G, Fraser DD. Pediatric sepsis inflammatory blood biomarkers that correlate with clinical variables and severity of illness scores. J Inflamm (Lond). 2024;21(1):7.
11. Van Nynatten LR, Slessarev M, Martin CM, Leligdowicz A, Miller MR, Patel MA, Daley M, Patterson EK, Cepinskas G, Fraser DD. Novel plasma protein biomarkers from critically ill sepsis patients. Clin Proteom. 2022;19(1):50.
12. Buhimschi CS, Bhandari V, Han YW, Dulay AT, Baumbusch MA, Madri JA, Buhimschi IA. Using proteomics in perinatal and neonatal sepsis: hopes and challenges for the future. Curr Opin Infect Dis. 2009;22(3):235–43.
13. Sharma NK, Salomao R. Sepsis Through the eyes of proteomics: the progress in the last decade. Shock 2017;47(1S Suppl 1):17–25.
14. Wong HR, Cvijanovich N, Lin R, Allen GL, Thomas NJ, Willson DF, Freishtat RJ, Anas N, Meyer K, Checchia PA. Identification of pediatric septic shock subclasses based on genome-wide expression profiling. BMC Med. 2009;7(1):34.
15. Wong HR, Salisbury S, Xiao Q, Cvijanovich NZ, Hall M, Allen GL, Thomas NJ, Freishtat RJ, Anas N, Meyer K. The pediatric sepsis biomarker risk model. Crit Care. 2012;16(5):R174.
16. Wong HR. Genome-wide expression profiling in pediatric septic shock. Pediatr Res. 2013;73(2):564–9.
17. Wong HR, Cvijanovich NZ, Anas N, Allen GL, Thomas NJ, Bigham MT, Weiss SL, Fitzgerald JC, Checchia PA, Meyer K. Improved risk stratification in pediatric septic shock using both protein and mRNA biomarkers. PERSEVERE-XP. Am J Respir Crit Care Med. 2017;196(4):494–501.
18. Cui M, Cheng C, Zhang L. High-throughput proteomics: a methodological mini-review. Lab Invest. 2022;102(11):1170–81.
19. Aleksander SA, Balhoff J, Carbon S, Cherry JM, Drabkin HJ, Ebert D, Feuermann M, Gaudet P, Harris NL. The gene ontology knowledgebase in 2023. Genetics. 2023;224(1):iyad031.
20. Fraser DD, Van Nynatten LR, Tweddell D, Daley M, Russell JA. Divergent biological pathways distinguish community-acquired pneumonia from COVID-19 despite similar plasma cytokine profiles. Respir Res. 2025;26(1):264.
21. Shi J, Walker MG. Gene set enrichment analysis (GSEA) for interpreting gene expression profiles. Curr Bioinform. 2007;2(2):133–7.
22. Goldstein B, Giroir B, Randolph A, International Consensus Conference on Pediatric S. International pediatric sepsis consensus conference: definitions for sepsis and organ dysfunction in pediatrics. Pediatr Crit Care Med. 2005;6(1):2–8.
23. Schlapbach LJ, Watson RS, Sorce LR, Argent AC, Menon K, Hall MW, Akech S, Albers DJ, Alpern ER, Balamuth F. International consensus criteria for pediatric sepsis and septic shock. JAMA. 2024;331(8):665–74.
24. Brisson AR, Matsui D, Rieder MJ, Fraser DD. Translational research in pediatrics: tissue sampling and biobanking. Pediatrics. 2012;129(1):153–62.
25. Gillio-Meina C, Cepinskas G, Cecchini EL, Fraser DD. Translational research in pediatrics II: blood collection, processing, shipping, and storage. Pediatrics. 2013;131(4):754–66.
26. Lundberg M, Eriksson A, Tran B, Assarsson E, Fredriksson S. Homogeneous antibody-based proximity extension assays provide sensitive and specific detection of low-abundant proteins in human blood. Nucleic Acids Res. 2011;39(15):e102.
27. Assarsson E, Lundberg M, Holmquist G, Björkesten J, Thorsen SB, Ekman D, Eriksson A, Rennel Dickens E, Ohlsson S, Edfeldt G, et al. Homogenous 96-plex PEA immunoassay exhibiting high sensitivity, specificity, and excellent scalability. PLoS ONE. 2014;9(4):e95192.
28. Breiman LRML. Random forests. Mach Learn. 2001;45(1):5–32.
29. Geurts P, Ernst D, Wehenkel L. Extremely randomized trees. Mach Learn. 2006;63:3–42.
30. Friedman JH. Greedy function approximation: a gradient boosting machine. Ann Stat. 2001;29:1189–232.
31. Kursa MB, Rudnicki WR. Feature selection with the Boruta package. J Stat Softw. 2010;36:1–13.
32. Grissa D, Junge A, Oprea TI, Jensen LJ. Diseases 2.0: a weekly updated database of disease-gene associations from text mining and data integration. Database (Oxford) 2022, 2022.
33. Madsen EC, Levy ER, Madden K, Agan AA, Sullivan RM, Graham DA, Randolph AG. Mannose-binding lectin levels in critically ill children with severe infections. Pediatr Crit Care Med. 2017;18(2):103–11.
34. Inwald DP, Canter R, Woolfall K, Mouncey P, Zenasni Z, O'Hara C, Carter A, Jones N, Lyttle MD, Nadel S, et al. Restricted fluid

bolus volume in early septic shock: results of the Fluids in Shock pilot trial. Arch Dis Child. 2019;104(5):426–31.
35. Farris RW, Weiss NS, Zimmerman JJ. Functional outcomes in pediatric severe sepsis: further analysis of the researching severe sepsis and organ dysfunction in children: a global perspective trial. Pediatr Crit Care Med. 2013;14(9):835–42.
36. Ayar G, Atmaca YM, Alışık M, Erel Ö. Effects of paraoxonase, arylesterase, ceruloplasmin, catalase, and myeloperoxidase activities on prognosis in pediatric patients with sepsis. Clin Biochem. 2017;50(7–8):414–7.
37. Messerer DAC, Datzmann T, Baranowsky A, Peschel L, Hoffmann A, Gröger M, Amling M, Wepler M, Nussbaum BL, Jiang S, et al. Systemic calcitonin gene-related peptide receptor antagonism decreases survival in a porcine model of polymicrobial sepsis: blinded randomised controlled trial. Br J Anaesth. 2022;128(5):864–73.
38. Perlin DS, Neil GA, Anderson C, Zafir-Lavie I, Raines S, Ware CF, Wilkins HJ. Randomized, double-blind, controlled trial of human anti-LIGHT monoclonal antibody in COVID-19 acute respiratory distress syndrome. J Clin Invest 2022, 132(3).
39. Shi R, Wang J, Zhang Z, Leng Y, Chen AF. ASGR1 promotes liver injury in sepsis by modulating monocyte-to-macrophage differentiation via NF-κB/ATF5 pathway. Life Sci. 2023;315:121339.
40. Mierzchała-Pasierb M, Lipińska-Gediga M. Sepsis diagnosis and monitoring - procalcitonin as standard, but what next? Anaesthesiol Intensive Ther. 2019;51(4):299–305.
41. Mota RF, Cavalcanti de Araújo PH, Cezine MER, Matsuo FS, Metzner RJM, Oliveira de Biagi Junior CA, Peronni KC, Hayashi H, Shimamura M, Nakagami H, et al. RANKL Impairs the TLR4 Pathway by Increasing TRAF6 and RANK Interaction in Macrophages. Biomed Res Int. 2022;2022:7740079.
42. Roderburg C, Benz F, Schüller F, Pombeiro I, Hippe HJ, Frey N, Trautwein C, Luedde T, Koch A, Tacke F, et al. Serum levels of TNF receptor ligands are dysregulated in sepsis and predict mortality in critically ill patients. PLoS ONE. 2016;11(4):e0153765.
43. Lecaille F, Chazeirat T, Saidi A, Lalmanach G. Cathepsin V: Molecular characteristics and significance in health and disease. Mol Aspects Med. 2022;88:101086.
44. Kaczynski TJ, Husami NJ, Au ED, Farkas MH. Dysregulation of a lncRNA within the TNFRSF10A locus activates cell death pathways. Cell Death Discov. 2023;9(1):242.
45. Yin C, Fu L, Guo S, Liang Y, Shu T, Shao W, Xia H, Xia T, Wang M. Senescent fibroblasts drive FAP/OLN imbalance through mTOR signaling to exacerbate inflammation and bone resorption in periodontitis. Adv Sci (Weinh). 2025;12(7):e2409398.
46. Yang AT, Kim YO, Yan XZ, Abe H, Aslam M, Park KS, Zhao XY, Jia JD, Klein T, You H, et al. Fibroblast activation protein activates macrophages and promotes parenchymal liver inflammation and fibrosis. Cell Mol Gastroenterol Hepatol. 2023;15(4):841–67.
47. Iwaszko M, Biały S, Bogunia-Kubik K. Significance of interleukin (IL)-4 and IL-13 in inflammatory arthritis. Cells 2021;10(11).
48. Kobayashi M, Tsuda Y, Yoshida T, Takeuchi D, Utsunomiya T, Takahashi H, Suzuki F. Bacterial sepsis and chemokines. Curr Drug Targets. 2006;7(1):119–34.
49. Wei H, Wang G, Tian Q, Liu C, Han W, Wang J, He P, Li M. Low shear stress induces macrophage infiltration and aggravates aneurysm wall inflammation via CCL7/CCR1/TAK1/ NF-κB axis. Cell Signal. 2024;117:111122.
50. Hoppe JE, Wagner BD, Kirk Harris J, Rowe SM, Heltshe SL, DeBoer EM, Sagel SD. Effects of ivacaftor on systemic inflammation and the plasma proteome in people with CF and G551D. J Cyst Fibros. 2022;21(6):950–8.
51. Aderka D. The potential biological and clinical significance of the soluble tumor necrosis factor receptors. Cytokine Growth Factor Rev. 1996;7(3):231–40.
52. Nedeva C. Inflammation and cell death of the innate and adaptive immune system during sepsis. Biomolecules 2021;11(7).
53. Chousterman BG, Swirski FK, Weber GF. Cytokine storm and sepsis disease pathogenesis. Semin Immunopathol. 2017;39(5):517–28.
54. Fan Y, Moser J, van Meurs M, Kiers D, Sand JMB, Leeming DJ, Pickkers P, Burgess JK, Kox M, Pillay J. Neo-epitope detection identifies extracellular matrix turnover in systemic inflammation and sepsis: an exploratory study. Crit Care. 2024;28(1):120.
55. Gäddnäs F, Koskela M, Koivukangas V, Risteli J, Oikarinen A, Laurila J, Saarnio J, Ala-Kokko T. Markers of collagen synthesis and degradation are increased in serum in severe sepsis: a longitudinal study of 44 patients. Crit Care. 2009;13(2):R53.
56. Gäddnäs FP, Koskela M, Koivukangas V, Laurila J, Saarnio J, Risteli J, Oikarinen A, Ala-Kokko T. Skin collagen synthesis is depressed in patients with severe sepsis. Anesth Analg. 2010;111(1):156–63.
57. Liu Z, Ting Y, Li M, Li Y, Tan Y, Long Y. From immune dysregulation to organ dysfunction: understanding the enigma of Sepsis. Front Microbiol. 2024;15:1415274.
58. Foster DM, Kellum JA. Endotoxic septic shock: diagnosis and treatment. Int J Mol Sci 2023;24(22).
59. Gopallawa I, Dehinwal R, Bhatia V, Gujar V, Chirmule N. A four-part guide to lung immunology: invasion, inflammation, immunity, and intervention. Front Immunol. 2023;14:1119564.
60. Sankar J, Thakral V, Bharadwaj K, Agarwal S, Kabra SK, Lodha R, Rathore S. The microbiome and metabolome of the gut of children with sepsis and septic shock. J Intensive Care Med. 2024;39(6):514–24.
61. Qin Y, Caldino Bohn RI, Sriram A, Kernan KF, Carcillo JA, Kim S, Park HJ. Refining empiric subgroups of pediatric sepsis using machine-learning techniques on observational data. Front Pediatr. 2023;11:1035576.
62. Cajander S, Kox M, Scicluna BP, Weigand MA, Mora RA, Flohé SB, Martin-Loeches I, Lachmann G, Girardis M, Garcia-Salido A, et al. Profiling the dysregulated immune response in sepsis: overcoming challenges to achieve the goal of precision medicine. Lancet Respir Med. 2024;12(4):305–22.
63. Lu J, Zhang W, He Y, Jiang M, Liu Z, Zhang J, Zheng L, Zhou B, Luo J, He C, et al. Multi-omics decodes host-specific and environmental microbiome interactions in sepsis. Front Microbiol. 2025;16:1618177.
64. Stranges V, Tweddell D, Cela E, Morello M, Daley M, Cepinskas G, Fraser DD. Differential protein expression and enriched pathways in pediatric sepsis: identification of novel brain-associated biomarkers revealed through proteomic profiling. Mol Med. 2025;32:14.
65. Koçak Tufan Z, Kayaaslan B, Mer M. COVID-19 and Sepsis. Turk J Med Sci. 2021;51(Si–1):3301–11.
66. Patel MA, Fraser DD, Daley M, Cepinskas G, Veraldi N, Grazioli S. The plasma proteome differentiates the multisystem inflammatory syndrome in children (MIS-C) from children with SARS-CoV-2 negative sepsis. Mol Med. 2024;30(1):51.

## Authors and Affiliations

**Vincenzo Stranges[1] · Logan R. Van Nynatten[2,3] · David Tweddell[4] · Enis Cela[3] · Maria Morello[5] · Mark Daley[4,6] · David B. O'Gorman[7] · Gediminas Cepinskas[8,9,10] · Douglas D. Fraser[3,10,11,12,13,14]**

✉ Douglas D. Fraser
douglas.fraser@lhsc.on.ca

1 Maternal and Child Health and Urological Sciences, Policlinico Umberto I, Rome, Italy

2 Critical Care Medicine, Western University, London, ON, Canada

3 Physiology and Pharmacology, Western University, London, ON, Canada

4 Computer Science, Western University, London, ON, Canada

5 Experimental Medicine, University of Rome Tor Vergata, Rome, Italy

6 Epidemiology and Biostatistics, Western University, London, ON, Canada

7 Biochemistry, Western University, London, ON, Canada

8 Medical Biophysics, Western University, London, ON, Canada

9 Anatomy and Cell Biology, Western University, London, ON, Canada

10 London Health Sciences Centre Research Institute, London, ON N6A 5W9, Canada

11 Pediatrics, Western University, London, ON, Canada

12 Clinical Neurological Sciences, Western University, London, ON, Canada

13 Children's Health Research Institute, London, ON, Canada

14 GSK Chair in Clinical Pharmacology, Western University, London, ON, Canada